JOURNAL OF AGRICULTURAL AND FOOD CHEMISTRY

Article

pubs.acs.org/JAFC

Nonionic Surfactant and Interfacial Structure Impact Crystallinity and Stability of β-Carotene Loaded Lipid Nanodispersions

Amir Malaki Nik, Sarah Langmaid, and Amanda J. Wright*

Department of Human Health and Nutritional Sciences, University of Guelph, Guelph, Ontario N1G 2W1, Canada

ABSTRACT: The stability, crystallization, and melting behavior of canola stearin (CaSt) solid lipid nanoparticle dispersions (SLN) and canola oil-in-water emulsions (COE) with 10 wt % Poloxamer 188 (P188) or Tween 20 (T20) with and without 0.1 wt % β-carotene (BC) were investigated. Particles or droplets with diameters in the range of 115 nm were formed and stable for up to 90 days at 4 or 20 °C. Polymorphism was affected by surfactant type; that is, only β versus both β′ and β were observed for the P188 and T20 SLN, respectively. According to Cryo-TEM, the emulsions and SLN were spherical versus platelet-like structures, respectively, with differences observed between SLN with P188 or T20. More surfactant was interfacially adsorbed in the SLN versus COE. Incorporation of BC at 0.1 wt % had no impact on SLN or COE size, polymorphism, or melting behavior. Less BC degradation was observed for the SLN versus COE and during storage at 4 versus 20 °C ($p < 0.05$).

KEYWORDS: *solid lipid nanoparticles, nonionic surfactants, particle size, crystallization, encapsulation, interfacial structure, β-carotene*

INTRODUCTION

Solid lipid nanoparticle dispersions (SLN) are crystallized emulsions with potential as delivery systems for lipophilic bioactive molecules.[1] Their small size (radius <100 nm),[2] lipidic nature, modifiable surface characteristics, and solid fat matrix all contribute to the protection of encapsulated molecules. The emulsifier present influences SLN formation, properties, stability, and ultimately their utility. This occurs not only through direct effects on particle size and charge, but also by impacting crystallization and polymorphic behavior of the matrix lipids.[3,4] In turn, SLN polymorphism influences loading capacity and stability.[5] Specifically, the minimally ordered α polymorph matrix has been associated with relatively high encapsulation efficiencies, but can destabilize during storage,[6] leading to compound expulsion and dispersion gelation. For example, 10 wt % tripalmitin SLN stabilized with 1.5 wt % Tween 20 (T20) quickly transformed from the α to the β form and gelled at 5 °C.[7] In 10 wt % canola stearin (CaSt) SLN, Poloxamer 188 (P188) (0.5−10 wt %) promoted transitions to the β polymorph, although gelation was not observed.[8] In this case, the α polymorph disappeared within 2 h of crystallization in SLN with 10 wt % P188 at 22 °C. The β crystalline structure is suggested to be too highly ordered and densely packed to incorporate guest molecules.[9−11] However, if encapsulation were possible, very early transition to the β polymorph in SLN dispersions might eliminate issues associated with unpredictable transitions.

Previous studies have indicated the importance of emulsifier type and chemical structure on SLN physical properties, including crystallization and melting behavior.[3,7,12] For example, droplets stabilized with high-melting surfactants (i.e., high-melting lecithin or Tween 60) crystallized at higher temperatures as compared to low-melting surfactants (i.e., low-melting lecithin or Tween 80)[12] and saturated versus unsaturated phospholipids, respectively, prevented versus promoted β formation, with the effects attributed to different interfacial structures.[5] Among the nonionic surfactants researched for SLN are the Tweens (polysorbates)[12,13] and Poloxamers.[8,14] Both types of surfactants prevent particle or droplet destabilization through steric repulsion. T20 is the most hydrophilic Tween with a hydrophilic−lipophilic balance (HLB) value of 16.7 and contains the fully saturated 12-carbon molecule lauric acid. Poloxamers are water-soluble triblock copolymers of polyethyleneoxide (PEO) and polypropyleneoxide (PPO), which differ in terms of molecular weight because of differences in the number of repeating hydrophilic PEO and hydrophobic PPO groups.[15] P188 contains 150 PEO groups surrounding 30 PPO repeats and has a molecular weight of 8350 g mol^{-1} and an HLB value of 29.[16]

The influence of nonionic surfactants on SLN formation and polymorphism, especially in relation to their ability to protect encapsulated molecules, requires further investigation. While a solid matrix confers stability, differences in bioactive stabilization can occur because of different interfacial properties and molecular chemistry.[17,18] The purpose of this research was to investigate the encapsulation and protection of BC, as a model lipophilic molecule, in CaSt SLN stabilized by two nonionic surfactants, that is, T20 and P188. The influence of BC encapsulation on SLN colloidal structures and properties and the importance of a solid matrix, by comparison with canola oil-in-water emulsions (COE), were also studied. Colloidal stability was assessed by visual observation and determination of size distributions and mean particle/droplet diameters. BC is a provitamin A molecule, the consumption of which has also been associated with decreased chronic disease risk.[19] However, low aqueous solubility, limited bioavailability, and sensitivity to heat and light are challenges with respect to its encapsulation and delivery.[20]

Received: November 22, 2011
Revised: March 6, 2012
Accepted: March 8, 2012
Published: March 8, 2012

MATERIALS AND METHODS

Materials. Fully hydrogenated CaSt was provided by Bunge Canada (Toronto, ON) and consisted of 84.6 wt % stearic acid, 8.6 wt % palmitic acid, 2.8 wt % oleic acid, and 1.7 wt % linoleic acid with a melting temperature of 69.9 ± 0.3 °C.[8] Canola oil was purchased from a local market (Guelph, ON, Canada) and contained 4.4 ± 0.4 wt % palmitic acid, 2.6 ± 0.1 wt % stearic acid, 72.1 ± 0.5 wt % oleic acid, 13.5 ± 0.02 wt % linoleic acid, and 6.4 ± 0.1 wt % linolenic acid. P188 (PEO-PPO-PEO triblock copolymer, melting temperature of 52−57 °C, also known as Pluronic F68) was supplied by BASF (Florham Park, NJ). T20 (polyoxyethylene sorbitan monolaurate), all *trans* BC, sodium azide, cobalt nitrate hexahydrate (>99.0%), and ammonium thiocyanate (99.9% metal basis) were purchased from Sigma-Aldrich (St. Louis, MO). Hexane (>95%, spectrophotometric grade), acetone (>99.5%, A.C.S. reagent), ethyl acetate (LC-MS Chromasolv), and anhydrous ethanol (A.C.S certified) were also obtained from Sigma-Aldrich, and methylene chloride was purchased from Fisher Scientific (Fair Lawn, NJ). Deionized (DI) water was used to prepare all solutions.

Solid Lipid Nanoparticle (SLN) and Canola Oil-in-Water Emulsion (COE) Preparation. Aqueous surfactant solutions were prepared by dispersing the P188 or T20 into DI water followed by stirring for 2 h at room temperature. Initial studies were performed to determine the surfactant concentration required to achieve small and monomodally distributed droplets and particles. Therefore, SLN and COE were initially prepared with 0%, 2%, 5%, 10%, and 12.5% surfactant, and size distributions and mean particle/droplet diameters were determined, as below. However, for the purposes of this Article, SLN-P188 and SLN-T20 refer to CaSt SLN stabilized with 10% P188 and T20, respectively, while COE-P188 and COE-T20 refer to canola oil emulsions stabilized with 10% P188 and T20, respectively. To prevent bacteria growth during storage, 0.02 wt % sodium azide was included. Prior to homogenization, the surfactant solutions were heated to 95 °C. The CaSt was melted in a 95 °C oven for 30 min to erase any crystal memory. SLN were prepared by dispersing 10 wt % melted CaSt into the hot aqueous surfactant solutions (∼95 °C). The mixture was prehomogenized using an Ultra Turax (Ika T18 Basic) stand homogenizer at 10 000 rpm for 30 s followed by three homogenization passes through a microfluidizer processor (M-110EH, Microfluidics, MA) at 69 MPa. The microfluidizer piping was maintained above the melting temperature of CaSt by submersion in a water bath maintained at a set point of 95 °C and by running boiling water through several times prior to homogenization. After homogenization, samples were immediately placed in 20 mL borosilicate glass vials (Fisher Scientific) in a dark incubator at 20 °C for 24 h to crystallize. For COE preparation, 10 wt % hot canola oil was homogenized with the surfactant solutions (95 ± 1 °C), as above. To prepare the SLN and COE containing BC, 0.1 wt % BC was accurately weighed and stirred into the molten CaSt or hot canola oil (95 ± 1 °C). This concentration of BC was lower than the upper solubility limit (0.15 wt %) of BC in oil at room temperature (20 ± 3 °C).[21] The solution was held in a 95 °C oven and stirred to fully dissolve the BC.

Storage Conditions. SLN and COE samples (10 mL) were stored at 4 or 20 °C (representing refrigeration and room temperatures) with no exposure to light or air (except for that in the headspace) until analysis. The samples were analyzed for particle size, polymorphism, melting behavior, and BC degradation on days 1, 7, 28, and 90.

Assessment of Particle Stability, Size, and ζ-Potential Measurements. Samples were visually inspected for evidence of phase separation. Stability was also assessed on the basis of particle and droplet size distributions, volume-weighted mean diameter ($D_{4,3} = (\sum n_i d_i^4/\sum n_i d_i^3)$), and average surface-weighted diameters $D_{3,2} = (\sum n_i d_i^3/\sum n_i d_i^2)$, where n_i is the number of particles and d_i is the diameter of particles, as determined by laser diffraction (LD) using a Mastersizer 2000S (Malvern Instruments, UK). Hydrodynamic diameter (D_h) and ζ-potential values were determined by dynamic light scattering (DLS) using a Zetasizer Nano (Malvern Instruments, UK). Samples were diluted (∼1:100) in a 5 mM sodium phosphate buffer with a pH of 6.5. For both LD and DLS measurements, refractive indices of 1.47 and 1.33 were used for the dispersed phase and dispersant (DI water), respectively. All measurements were conducted at a constant temperature of 25 °C.

Cryogenic Transmission Electron Microscopy (Cryo-TEM). Solid particle and liquid droplet shape were determined using Cryo-TEM (FEI Tecnai G2 F20). Samples were prepared by applying 5 μL of diluted sample (1:15) onto a copper grid covered with holey carbon film (Quantifoil, Germany). The samples were blotted automatically between two strips of vitrobot FEI filter paper for 1.5 s and subsequently plunged into liquid ethane (∼ −180 °C). Samples were then placed in a precooled sample holder and transferred into the precooled Cryo-TEM unit, which was operated at 200 kV and −175 ± 1 °C. The images were recorded and analyzed with a Gatan 4k CCD camera and digital micrograph software.

Determination of Surfactant Aqueous Phase Concentration and Surface Load. Surfactant surface load (Γ_s) was calculated according to $\Gamma_s = C_a D_{3,2}/6\Phi$, where C_a is the mass of emulsifier adsorbed to the surface per unit volume of sample, $D_{3,2}$ is the volume-surface mean diameter, and Φ is the dispersed phase volume fraction (i.e., 0.1 CaSt or canola oil).[22] C_a was calculated by subtracting the amount of surfactant present in the aqueous phase from the initial amount of total surfactant. Aliquots of SLN and COE stabilized with P188 or T20 were centrifuged at 144 800*g* for 24 h at 7 °C, and the aqueous phase was separated using a fine-tip transfer pipet before filtering with a 0.1 μm filter. The colorimetric assay used for T20 determination was described elsewhere.[23] Briefly, aliquots (2 mL) of the aqueous phase were dried at 80 °C under nitrogen (N-evap Organomation, Berlin, MA). The sample was then cooled, and 0.4 mL of ammonium cobaltothiocyanate (ACTC) reagent and 0.8 mL of methylene chloride were added. The ACTC reagent was prepared using 3 g of cobalt nitrate hexahydrate and 18 g of ammonium thiocyanate in 100 mL of water. Samples were vortexed for 5 s and centrifuged at 10 400*g* for 10 min (5418 laboratory centrifuge, Eppendorf Hamburg, Germany). Following centrifugation, the methylene chloride layer was transferred to a glass microcuvette, and the absorbance at 620 nm was measured in a Hewlett-Packard 8451A Diode Array spectrophotometer. The amount of P188 present in the aqueous phase was determined as previously.[8] In brief, 200 μL of aqueous phase was mixed with 100 μL of ACTC reagent, 200 μL of ethyl acetate, and 80 μL of ethanol. The mixture was centrifuged at 10 400*g* for 1 min (5418 laboratory centrifuge, Eppendorf Hamburg, Germany). The upper liquid layer was removed, and the pellet was washed with ethyl acetate three times (i.e., until colorlessness was achieved). The pellet was dissolved in 2 mL of fresh acetone, and the absorbance at 624 nm was determined. The amount of P188 and T20 present in the aqueous phase was calculated using standard curves ranging from 0.0625 to 0.5 and 0.0065−0.1 wt % for P188 and T20 (r^2 = 0.99 for both), respectively. Samples were diluted with DI water prior to the reactions, where required.

Determination of BC Concentration. Details of the BC quantification are available elsewhere.[24] Briefly, samples were subjected to solvent extraction in which 0.5, 3, and 1 mL of ethanol, acetone, and DI water, respectively, were added with 5 s of vortexing after each addition. Two milliliters of hexane was added, and the organic layer was then removed using a glass transfer pipet. The hexane extraction was performed in triplicate, and the organic phase was then dried under nitrogen at 37 °C until the point of dryness when it was resolubilized in hexane and vortexed for 5 s. The absorbance at 450 nm was determined using a Hewlett-Packard 8451A Diode Array spectrophotometer. Beer's law and an extinction coefficient of 137 400 mol^{-1} cm^{-1} were used to calculate the BC concentration.

Powder X-ray Diffraction (XRD) Measurements. XRD measurements were carried out using a MultiFlex X-ray diffractometer (Rigaku, Japan) operated at 40 kV and 44 mA with Cu as the X-ray source (λ = 1.54 Å) and angle slits of 0.5°, 0.5°, and 0.3 mm. Approximately 1 mL of sample was pippetted into the well of a glass XRD slide. Scans were performed from 1° to 30° at 0.5° per min, while samples were maintained at 20 °C using a Peltier plate mounted beneath the sample holder. Peak positions were determined according to Bragg's Law using MID's Jade 6.5 software (Rigaku, Japan) and

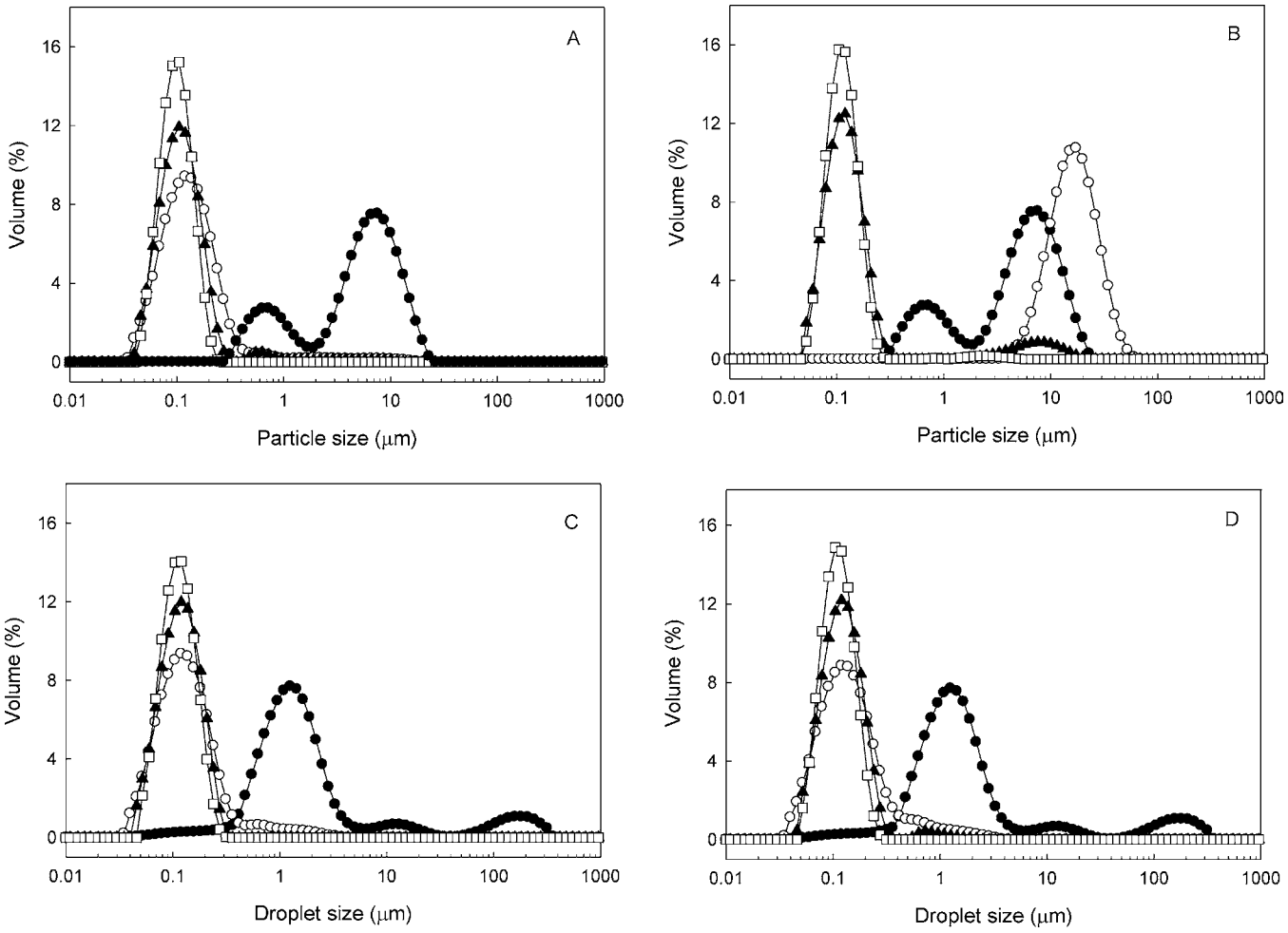

Figure 1. Particle size distributions of SLN-P188 (A), SLN-T20 (B), COE-P188 (C), and COE-T20 (D), as a function of surfactant concentration: 0 (●), 2 (○), 5 (▲), and 10 (□) wt %. Graphs shown are representative of three replicate samples.

Table 1. Mean Particle or Droplet Sizes ($D_{4,3}$, $D_{3,2}$, and D_h, nm) and ζ-Potential (mV) Values of SLN and COE Stabilized with 10 wt % P188 or T20, with and without BC[a]

	SLN-P188	SLN-BC-P188	SLN-T20	SLN-BC-T20	COE-P188	COE-BC-P188	COE-T20	COE-BC-T20
$D_{4,3}$	128.7 ± 1.1 ab	131.1 ± 0.1 a	126.0 ± 6.3 b	126.0 ± 0.1 b	127.0 ± 1.4 b	126.5 ± 0.0 b	127.0 ± 0.2 b	126.3 ± 0.2 b
$D_{3,2}$	115.3 ± 0.2 a	116.5 ± 0.0 a	112.6 ± 0.2 ab	112.6 ± 0.0 ab	111.7 ± 0.7 ab	112.0 ± 0.0 ab	111.7 ± 1.4 ab	110.3 ± 0.5 b
D_h	170.8 ± 3.6 a	176.4 ± 0.1 a	133.8 ± 0.5 b	145.6 ± 2.3 b	123.8 ± 6.2 c	121.3 ± 2.4 c	112.3 ± 0.7 d	113.4 ± 1.3 d
ζ-potential	−8.1 ± 2.0 d	−7.3 ± 0.7 d	−12.4 ± 2.7 a	−11.8 ± 2.3 a	−9.7 ± 1.9 b	−9.6 ± 0.6 b	−9.1 ± 0.8 c	−8.8 ± 0.5 c

[a]All measurements were performed after 24 h of dark storage at 20 °C. Values represent mean and standard deviation of three independent experiments. Within each row, different letters indicate significant difference at $p < 0.05$.

positions of 4.14, 3.8 and 4.2, and 4.6 Å were used to identify the α, β′, and β polymorphs, respectively.

Differential Scanning Calorimetry (DSC) Measurements. A Q1000 model DSC (TA Instruments, Mississauga, ON, Canada) was used to study the melting behavior of the bulk CaSt and SLN samples. Between 8−12 and 6−8 mg of dispersed SLN and bulk CaSt, respectively, were weighed and hermetically sealed in the same alodined aluminum pans. Samples stored at 20 °C were weighed into the pans at room temperature, while samples stored at 4 °C were prepared in a 5 ± 1 °C cold room. Samples were heated from their storage temperature (i.e., 4 or 20 °C) to 85 at 5 °C/min with an empty hermetically sealed alodined aluminum pan used as the reference. Instrument calibration was performed using indium as the standard. The instrument software, TA Universal Analysis (TA Instruments, Mississauga), was used to integrate the melting peaks and determine melting temperatures and enthalpies. Melting peaks were designated as the α, β′, or β polymorph on the basis of previous reports.[8]

Pulsed Nuclear Magnetic Resonance (pNMR) Measurements. A Bruker mq 20 minispec analyzer (Bruker Optics, Germany) was used to determine SLN solid fat content (SFC) after crystallization for 24 h at 20 °C. Approximately 5 mL of each sample was placed in glass NMR tubes, and triplicate measurements were made.

Statistical Analysis. All results were analyzed using two-way ANOVA and Duncan multiple comparisons testing with SAS software version 9.1 (SAS Institute Inc., NC). Data are the average of at least three independent experiments, and significance was considered at $p < 0.05$.

RESULTS AND DISCUSSION

Effect of Surfactant Concentration on Colloid Size. This work aimed to compare between samples with equivalent particle and droplet size. Therefore, the amount of surfactant

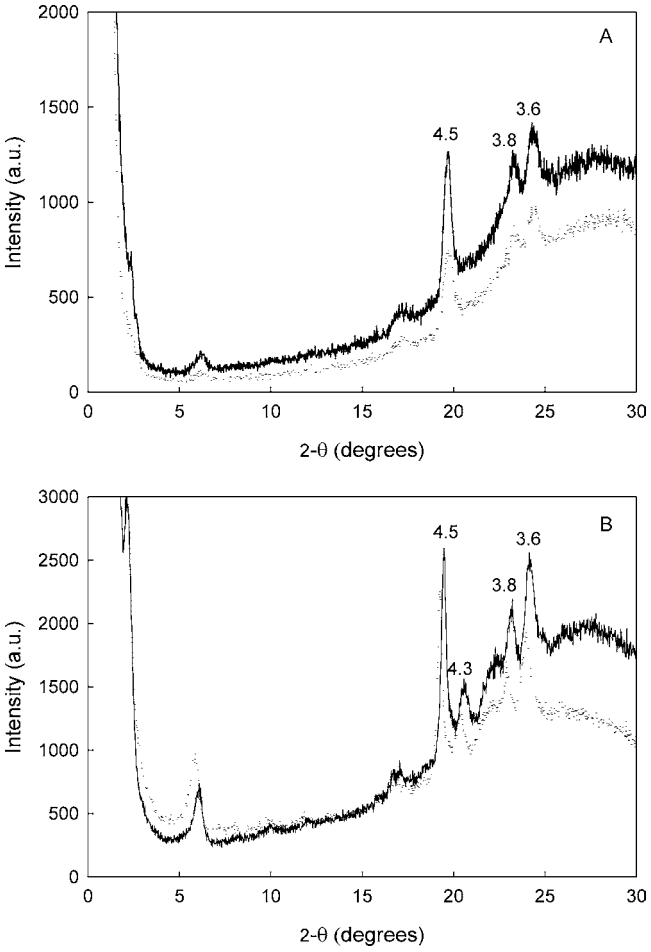

Figure 2. Representative X-ray diffractograms of SLN-P188 (A) and SLN-T20 (B) without BC (solid line) and with BC (dotted line). Spacings shown are in units of angstroms and were calculated from the 2θ refractive angle using Bragg's law.

(P188 or T20) required to achieve monomodally distributed and equivalent colloidal sizes for the SLN and COE was first determined. Figure 1 shows that more narrow size distributions and decreases in $D_{4,3}$ values were observed for the COE and SLN with up to 10 wt % P188 or T20 (data not shown, $p < 0.05$). No further reductions in mean droplet or particle diameter were observed using 12.5 wt % P188 or T20 for either the SLN or the COE (data not shown). Thus, subsequent results and discussion are based on SLN and COE stabilized with 10 wt % surfactant.

Physical Properties of SLN and COE Stabilized with 10 wt % Surfactant. Table 1 compares the mean $D_{4,3}$, $D_{3,2}$, and D_h values of the SLN and COE stabilized with 10 wt % P188 or T20 with and without BC. $D_{4,3}$ and $D_{3,2}$ values ranged from 126.3 to 131.1 and 110.3 to 116.5 nm, respectively. Although bioactive incorporation can influence SLN properties, as shown in Table 1, there was no impact of 0.10 wt % BC on particle or droplet diameter ($p > 0.05$). BC (0.025−0.20 mol fraction, i.e., 0.014−0.1 wt % total) was previously found to influence the optimal formulation and process conditions for stearic acid SLN containing lecithin, sodium taruocholate, and cholesterol.[25]

Interfacially adsorbed layers of T20 are reportedly thin, with the molecule having a headgroup of approximately ∼1.4 nm.[26] At an interface, P188's hydrophilic PEO groups extend into the aqueous, providing a highly hydrated, brush-like stabilizing layer,[16] the thickness of which depends on the nature of the dispersed phase.[27] The SLN-P188 (with and without BC) had slightly higher $D_{4,3}$ and $D_{3,2}$ values than the rest of the samples ($p < 0.05$). D_h values for SLN with P188 and T20 were also higher than the corresponding emulsions ($p < 0.05$), indicating more drag from the surfactant layer. As with the T20 versus P188 comparison, the higher D_h values suggest the presence of an interfacial layer, which protrudes into solution more with the SLN versus emulsions.

Table 1 shows that slightly negative ζ-potential values were observed for the SLN and COE stabilized with P188 or T20, both in the absence and in the presence of BC (at pH 6.5). Similar negative charges for nonionic surfactants at near neutral pH have been related to interactions of water molecule hydroxyl (OH) groups with cationic impurities in the surfactants.[25] The presence of BC in the SLN or COE had no impact on ζ-potential. This is in line with evidence that BC tends to distribute within the core of an oil droplet, with no effect on surface properties.[28] Differences in ζ-potential were observed between the droplets and particles for both surfactants ($p < 0.05$), although the trends were different and the magnitude of the differences small. The SLN-T20 had the largest ζ-potential value (i.e., -12.4 ± 2.7 mV, Table 1, $p < 0.05$) of the systems studies, including the COE-T20. This larger ζ-potential value is consistent with the presence of a greater number of impurities at the solid versus liquid interface. It suggests there was more interfacially located T20 in the SLN, which might have occurred because of surfactant entrapment within the crystallizing triacylglycerols (TAG), as discussed below.

Droplet and Particle Stability. Changes in particle and droplet diameter during 90 day dark storage at 4 and 20 °C were investigated as an indicator of colloidal stability. No increases in $D_{3,2}$ and $D_{4,3}$ were observed for the SLN and COE with T20 (data not shown, $p > 0.05$). Similarly, SLN and COE stabilized with P188 were also stable up to 90 days with $D_{3,2}$ values of ∼120 and 115 nm, respectively (data not shown, $p > 0.05$). The formation of a few large aggregates after 28 days was indicated by increases in $D_{4,3}$ at both temperatures, although agitation disrupted the flocs. Flocculation of P188-stabilized oil-in-water droplets was previously related to depletion-flocculation caused by nonadsorbed P188 micelles in the aqueous phase.[29] The critical micelle concentrations (CMC) of P188 and T20 are 1.2×10^{-4} M [30] and 4.88×10^{-5} M,[31] respectively. The relative sample stability is not surprising in light of the high surfactant concentrations. The 6 wt % T20 was found to minimize tripalmitin SLN destabilization by gelation, which was related to flocculation and coalescence because of underlying polymorphic transitions at lower surfactant concentrations.[7] The inclusion of 0.1 wt % BC did not appear to affect SLN or COE stability. Similarly, incorporation of 5 wt % of the lipophilic drug clotrimazole in tripalmitin SLN had no effect on particle size over 3 months.[32] There also was no clear impact of temperature on SLN stability in the present study. Significant particle growth was also not observed during 3 month storage at 4, 20, and 40 °C of tripalmitin SLN containing tyloxapol.[32]

Surfactant Aqueous Phase Concentrations and Surface Loads. P188 and T20 form micelles, especially at higher temperatures.[15,33] Therefore, the effective concentration available to adsorb to the newly created droplet interfaces during high temperature homogenization is lower than after cooling. This at least partly explains why excess surfactant is

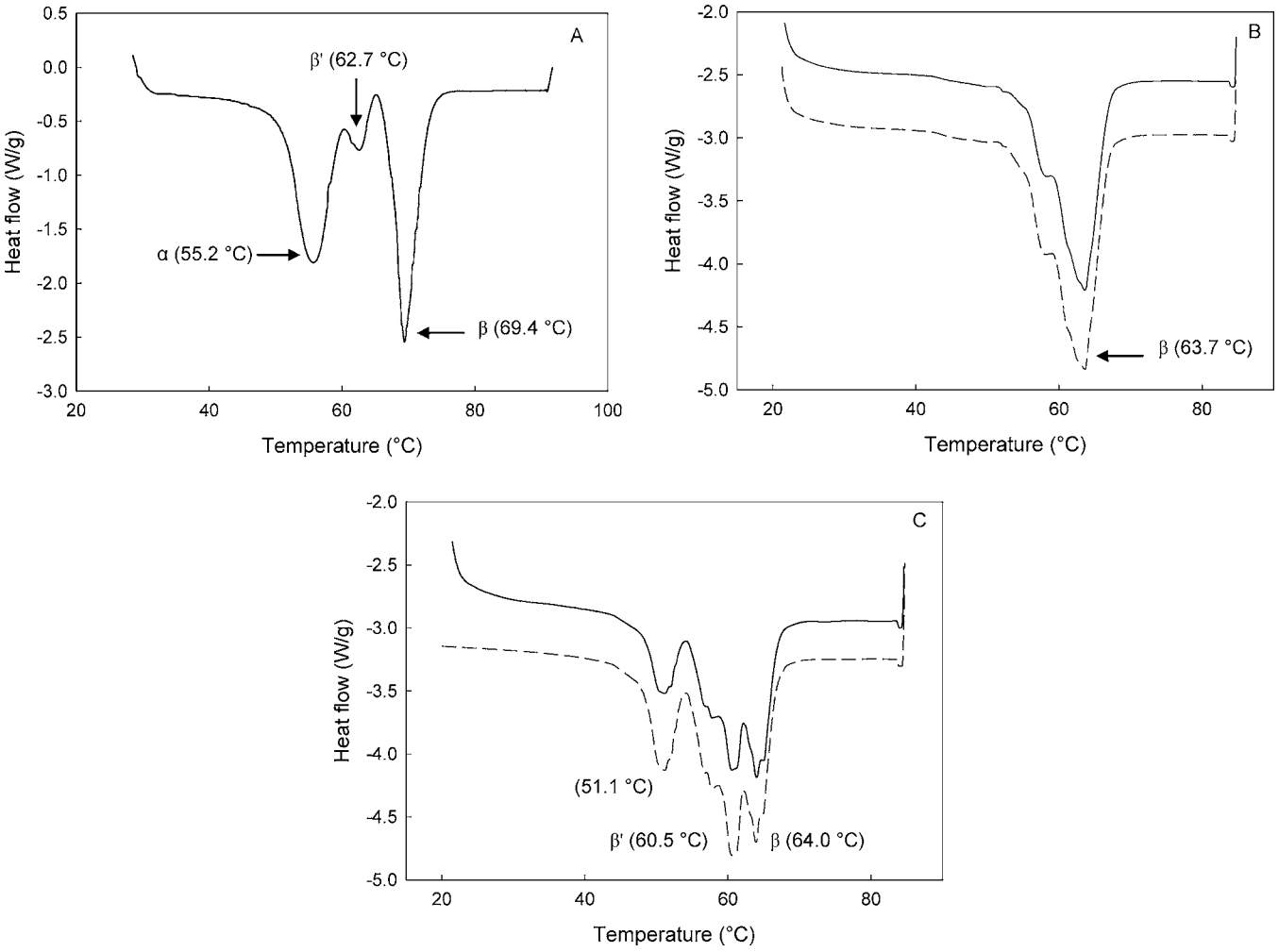

Figure 3. Representative DSC thermograms of bulk CaSt (A), SLN-P188 (B), and SLN-T20 (C) without BC (solid line) and with BC (dash line). All samples were crystallized at 20 °C for 24 h and melted from 20 to 85 at 5 °C/min.

required to form versus to stabilize these colloidal systems[7,8] and implies that a significant portion of surfactant may be present in the aqueous phase after production. Above 2 wt %, P188 was present in the aqueous phase of 10 wt % CaSt SLN.[8] Similarly, roughly 3.5 wt % total T20 was required to saturate the droplets of a 10 wt % tripalmitin emulsion.[13] In the present study, surfactant aqueous phase concentrations were 6 ± 0.2% (i.e., 7.2×10^{-3} M), 5.6 ± 0.2% (i.e., 4.1×10^{-2} M), 8.5 ± 0.1% (i.e.10.2×10^{-3} M), and 7.6 ± 0.3% (i.e., 5.7×10^{-2} M) for the SLN-P188, SLN-T20, COE-P188, and COE-T20, respectively, and all above the CMC, as previously stated. Therefore, more surfactant was present within the aqueous phase for the COE versus SLN, meaning there was more surfactant located at the interface of the solid particles versus oil droplets. Surfactant surface loads of 2.9 ± 0.2 and 4.4 ± 0.5 mg m^{-2} were calculated for the COE-P188 and COE-T20, respectively ($p < 0.05$). Of note, P188 has a much higher average molecular weight (i.e., 8350 g mol^{-1}) than T20 (i.e., 1227 g mol^{-1}). Therefore, even at equivalent surface coverage values, more molecules of T20 versus P188 would be adsorbed. Surfactant surface loads could not be determined for the SLN samples based on the lack of sphericity (discussed below). However, there clearly is more P188 and T20 associated with the particles than the droplets. Differences in the amount of T20 needed to saturate a solid versus liquid interface have been related to shape differences.[13,34,35] A maximum T20 surface coverage of around 2 wt % was reported previously for 10 wt % liquid oil emulsions, whereas up to ∼3.6 wt % T20 associated with the interface of solidified particles. In the same study, decreases in the T20 aqueous phase concentration were specifically observed upon droplet crystallization.[13]

Lipid Phase Crystallinity, Polymorphism, and Melting Behavior. Representative X-ray diffractograms of the SLN stabilized with P188 or T20, both with and without BC, are shown in Figure 2. The SLN-P188 contained only the β polymorph after 24 h crystallization at 20 °C (Figure 2A). In contrast, the SLN-T20 contained both the β' and β polymorphs (Figure 2B). These differences may be related to different interfacial dynamics, because emulsifier type can have a significant impact on SLN polymorphism. The presence of a fatty acid moiety is particularly relevant. For example, when stabilizers that contained a fatty acid moiety were present, multiple crystallization events were observed for cholesteryl myristate nanoparticles, indicating interactions with the dispersed phase TAG. The same was not observed when polymer-type stabilizers that did not contain a fatty acid were used.[36] In another example, polyvinyl alcohol kinetically stabilized the α polymorph (delayed β formation) in tristearin SLN,[10] with the effect attributed to steric hindrance because of

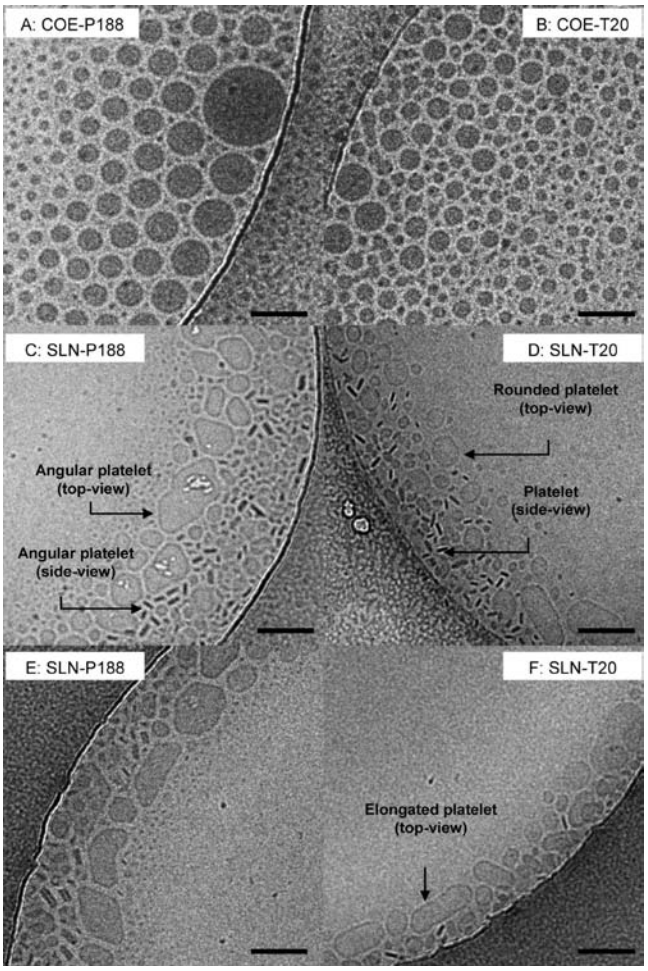

Figure 4. Cryo-TEM micrographs of COE-P188 (A), COE-T20 (B), SLN-P188 (C and E), and SLN-T20 (D and F). Scale bars represent 200 nm.

viscosity or molecular immobilization effects, rather than direct interactions between the stabilizer and crystallizing TAG.

P188 was previously found to promote transformation to the β polymorph, both directly through interacting with the crystallizing CaSt TAG (i.e., surface nucleation) and indirectly through SLN size reduction effects.[8] In the absence of P188, particles (of similar size) were exclusively in the α form. Addition of only 0.5 wt % P188 to the hot emulsion prior to crystallization led to the presence of β (with α) after 24 h, and no α was detected at 10 wt % surfactant.[8] Therefore, P188 acts, at least in part, to seed crystallization.[8] At sufficient concentrations, some Tweens have been shown to delay polymorphic transitions in SLN. For example, at 6 wt %, T20 prevented the rapid α to β transition that occurred at 5 °C in tripalmitin SLN with only 1.5 w %.[3,7] This occurred through the formation of a rigid surfactant shell that entrapped the solid droplet.[13] Tween 60, which is solid at room temperature (melting temperature ~57 °C), also stabilized the α polymorph in the presence of the β' and β forms in tripalmitin SLN after 24 h.[12] In contrast, Tween 80, which is liquid at room temperature, was associated with the presence of only β' and β.[12] The differences were attributed to effects of surface nucleation promoted by the Tween 60 based on its high melting temperature. However, the same explanation cannot account for the stabilization observed with T20 in the present study because it is also liquid at room temperature. Instead, we postulate that the presence of lauric acid in T20 permits associations between the TAG and surfactant at the interface in the liquid state and leads to entrapment within the crystalline matrix during the rapid TAG crystallization. The presence of T20 within the crystal structure at the interface then conceivably prevents the tighter packing and higher TAG ordering associated with the transition to β, resulting in apparent β' stability.

Figure 3 shows the DSC melting profiles of bulk CaSt and the SLN stabilized with P188 or T20 with and without BC. Three distinct peaks, corresponding to melting points of the α, β', and β polymorphs, were observed in bulk CaSt at 55.2 ± 0.5, 62.7 ± 0.4, and 69.4 ± 0.3 °C, respectively (Figure 3A), and in agreement with previous reports.[8] The SLN-P188 had only one melting event at 63.7 ± 0.1 °C, corresponding to melting of the β form and in agreement with the XRD data (Figure 2A). In contrast, the SLN-T20 had two distinct melting peaks at 60.5 ± 0.1 and 64.0 ± 0.1 °C, corresponding to the β' and β forms, respectively (Figure 3C). In agreement with previous reports,[9] the melting temperatures for the SLN β forms were approximately 5 °C lower than for bulk lipid. The β melting temperature was higher for the SLN-T20 versus SLN-P188 ($p < 0.05$). Assuming equivalent particle size, this indicates that T20 and P188 impact TAG melting through different compositional and or structural effects, although the difference is very small (i.e., 63.7 ± 0.1 versus 64.0 ± 0.1 °C).

A third melting peak was present in the SLN-T20 at 51.1 ± 0.2 °C. According to XRD (Figure 2B), there was no evidence of the α polymorph, and attempts to experimentally observe the α form in the SLN-T20 were unsuccessful. Also, when a 10 wt % T20 solution was heated from 25 to 80 at 5 °C per min, there was no melting event (data not shown). These results further support that T20 and P188 interact differently at the oil–water interface and that the presence of T20 increased the complexity of the TAG crystal structure. Helgason et al.[13] observed that, while at low concentration, the lauric acid tails of T20 packed loosely at an oil–water interface, and at higher concentrations, the tails packed more tightly and behaved more solid-like, leading to more complex melting profiles.

Incorporation of 0.1 wt % BC had no effect on polymorphism by XRD or SLN peak melting temperature (Figures 2, 3B and C, $p > 0.05$), perhaps because of the low concentration utilized (i.e., 0.1 wt %). This concentration was selected to be below BC's solubility limits, and a melting peak corresponding to crystallized BC (melting temperature 181 ± 1 °C) was not expected nor observed (data not shown). Incorporation of 0.035 wt % BC in a nanostructured lipid (consisting of propylene glycol monostearate and sunflower oil stabilized with Tween 80)[37] or 0.1% diazepam in tristearin SLN stabilized with poly vinyl alcohol[10] also did not change the polymorphic or melting behaviors. Incorporation of up to 70 wt % coenzyme Q_{10} (CoQ_{10}, melting temperature of 48 °C) in tripalmitin SLN also had no effect on XRD pattern peak position.[38] However, XRD peak intensity decreased with increasing CoQ_{10} concentration, to the point that, at 50 wt % CoQ_{10}, no peaks were observed at room temperature, suggesting the absence of solid fat[38] and eutectic behavior. Eutectic behavior was also reported for palm oil SLN at different lecithin concentrations.[39] In this study, a high degree of crystallinity was observed for the SLN-P188 and SLN-T20 (i.e., solid fat content 12.4 ± 0.1%, data not shown, $p > 0.05$). Of note, this is slightly higher than anticipated given that the

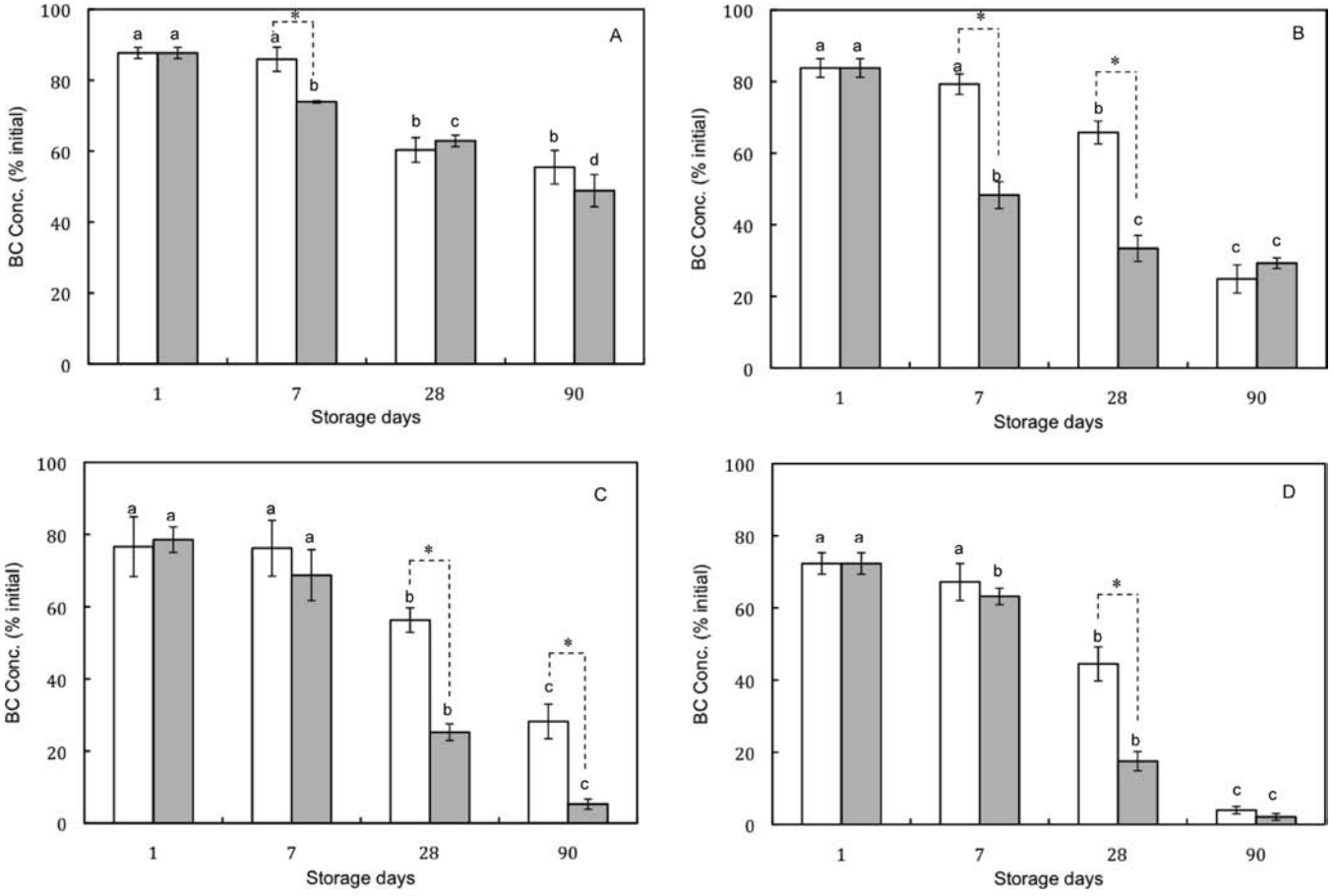

Figure 5. BC concentration (% of initial, where initial refers to after homogenization) in SLN-P188 (A), SLN-T20 (B), COE-P188 (C), and COE-T20 (D) during 90 days of dark storage at 4 (empty bars) and 20 °C (filled bars). Error bars represent mean ± standard deviation for three independent experiments. Within each storage temperature, different letters (a–d) indicate significant difference over 90 days at $p < 0.05$. Within each storage day, "*" indicates significant difference at $p < 0.05$.

SLN contained 10 wt % CaSt, which had a bulk solid fat content of 99.0 ± 0.1% at 20 °C.[8] The discrepancy is likely attributable to interference by excess surfactant in the aqueous phase. Nevertheless, it can be concluded that the extent of crystallization was high for all samples and that the SLN were not supercooled melts.

Polymorphic transitions in crystallized droplets could lead to expulsion and/or degradation of encapsulated bioactive molecules.[12] Therefore, changes in SLN crystalline properties during 90 days storage at 4 and 20 °C were monitored. As expected, the SLN-P188 remained in the β polymorph, that is, the most stable form, throughout the study, whereas both β' and β were consistently present in the SLN-T20. There were no apparent changes in XRD peak intensity or in terms of β peak melting temperature over time (data not shown, $p > 0.05$). For the SLN-P188, β peak enthalpies were also compared. No differences were observed with the presence or absence of BC initially (i.e., 18.4 ± 0.2 and 18.9 ± 0.5 J g^{-1}, respectively, $p > 0.05$) or over time (data not shown). Peak enthalpies could not be compared for the SLN-T20, given the existence of multiple polymorphs and likelihood that some β' fat would transition to the β form upon heating in the DSC. However, the results support the conclusion that BC does not impact the stability of SLN prepared with either nonionic surfactant.

Morphology of Solid Particles and Liquid Droplets. Figure 4 shows that differences were observed between the liquid droplets and crystallized particles. As expected, the COE droplets were spherical, irrespective of the type of nonionic surfactant present (Figure 4). In addition, the approximate size of the droplets observed by microscopy was in good agreement with size distributions reported in Figure 1. In contrast, the SLN samples were not spherical. Rather, they contained heterogeneous mixtures of larger anisometrically shaped (top-view) and rod-like (side-view) structures, which is in accordance with the appearance of platelets observed from different views. These differences in shape help to explain the higher D_h values observed for the particles (platelets) versus droplets (spheres) (Table 1).

Emulsifier type can affect SLN morphology.[36] Trimyristin SLN with different emulsifiers were dominated by platelet-like anisometric shapes.[40] Also, the edges of Tween 80-stabilized platelets were reportedly smoother than the edges of particles stabilized with P188. Similarly, in the present study, the edges of the SLN-T20 (Figure 4D and F) were more rounded than the SLN-P188 (Figure 4C and E). Figure 4F shows the presence of some large cylindrically shaped particles in a sample of SLN-T20. These are similar to large oval-shaped cholesterol myristate particles, which were previously attributed to nanoparticle recrystallization in samples containing polysorbate 80.[36]

Differences in SLN morphology are often attributed to differences in polymorphism. For example, α versus β tristearin particles were spherically versus anisometrically shaped.[34] Helgason et al.[7] observed a rapid α to β transition which was

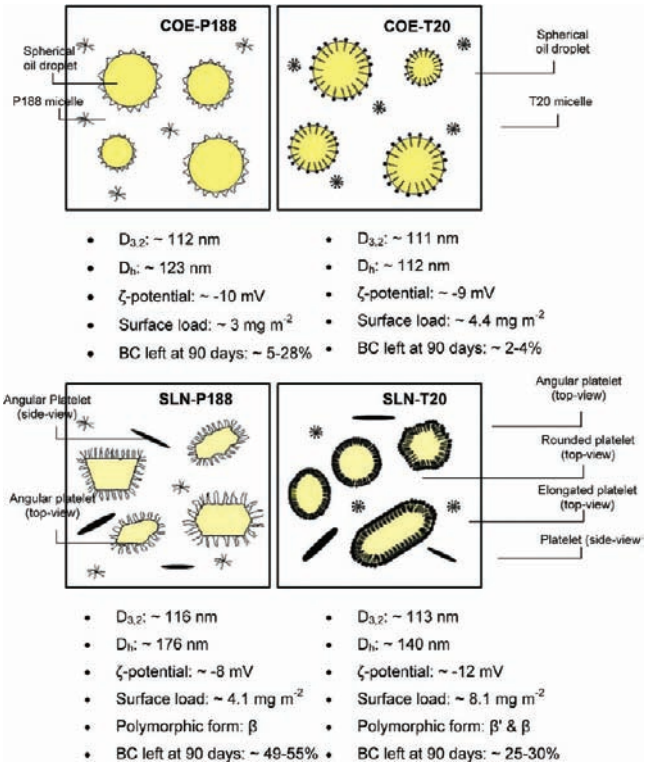

Figure 6. Schematic representation of COE and SLN stabilized with P188 or T20.

associated with shape changes and subsequent sample gelation in tripalmitin SLN with 1.5 wt % T20. In the present study, the SLN-P188 and SLN-T20 contained the β versus β' and β polymorphs, respectively. It was hypothesized that the existence of both β' and β in the SLN-T20 may have been related to separate populations of β' and β particles. However, most of the SLN-T20 structures have smooth, rounded edges (Figure 4D and F) in contrast to the SLN-P188 structures, which are less rounded in terms of their edging (Figure 4C and E). Because the SLN-P188 are exclusively in the β form, this suggests that the more rounded edges of the SLN-T20 may be related to the presence of β' closer to the interface, with the β polymorph located toward the SLN-T20 particle core.

Protection of Encapsulated BC. During production, 12−20% BC was lost during the initial heating of the lipid phases (i.e., 30 min at the 95 °C) (data not shown). This is in agreement with reports that around 20% of BC was degraded during heating at 97 °C for 1 h.[41] Microfluidization led to further losses, especially for the T20 samples (10 versus 5%) (Figure 5). Overall, total BC production losses of ∼16.3 ± 2.5%, 12.4 ± 1.5%, 21.4 ± 3.5%, and 27.7 ± 3.0% were observed for the SLN-T20, SLN-P188, COE-P188, and COE-T20, respectively ($p < 0.05$). Storage time and temperature, lipid physical state, and type of the surfactant all impacted BC long-term stability. The SLN-P188 had the highest BC retention (∼55%) at 90 days, with no impact of storage temperature observed for this system (Figure 5A). There was a marked reduction in BC in the SLN-T20 over time, especially with storage at 20 °C and within the first 28 days (Figure 5B). As compared to the solid particles, a gradual decrease in BC concentration was observed for the COE-P188, with the samples retaining more BC during storage at 4 °C (Figure 5C). The most extensive degradation was observed for the COE-T20; that is, only 2% BC remained after 90 days, regardless of storage temperature (Figure 5D).

BC retention was generally higher at 4 versus 20 °C and also for the solid particles versus liquid droplets, due to decreased oxidative degradation.[42] A solid matrix protects bioactives through decreased light exposure because of increases in light scattering related to increases in refractive index, and hence less photo-oxidation, as well as lower rates of diffusion of pro-oxidants into the lipid phase.[1] The impact of surfactant on oxidative stability of BC in solid particles has been reported previously.[12] SLN stabilized with high melting lecithin offered better protection than low melting lecithin, Tween 60, and Tween 80.[12] In the current study, surfactant effects were also observed in the crystallized systems; that is, BC losses were higher with T20 than P188 at both temperatures (compare Figure 5A and B). This is similar to the trends during SLN production. There were also differences between the SLN-T20 and SLN-P188 in terms of polymorphism, changes that have been related to bioactive degradation.[12] However, in this study, the highest BC stability was observed for the β-containing SLN-P188, with more extensive losses observed for the SLN-T20, which contained both β' and β. Of note, there also was no evidence by DSC or XRD of increasing amounts of the β form over time (data not shown).

Figure 6 summarizes the compositional and structural differences between the SLN and COE with T20 and P188. The results highlight the impact of nonionic emulsifier type on stability, crystallization, and melting behavior of SLN in relation to the potential to protect an encapsulated bioactive. Among other things, the properties of the interfacial layer surrounding an oil droplet can affect the rate of bioactive oxidation.[43] For example, controlling the interfacial charge and thickness improved the oxidative stability of ω-3 fatty acids by minimizing the interaction between the lipids and transition metal ions.[18] A more negatively charged interface, as was observed for the SLN-T20 versus SLN-P188, has a greater potential to attract counterions, including those of copper and iron, which might promote lipid oxidation.[18] There may also have been pro-oxidative impurities such as peroxides present in the T20,[18] leading to more extensive BC degradation. The differences between surfactant distribution suggest potentially higher viscosities in the interfacial regions of the solid particles overall and specifically for the SLN-P188 versus SLN-T20, which may have minimized the diffusion of reactive molecules. Last, the presence of surfactant micelles in the aqueous phase can also impact oxidative stability because of their ability to solubilize pro-oxidants and antioxidants.[18]

AUTHOR INFORMATION

Corresponding Author

*Tel.: (519) 824-4120 ext 54697. Fax: 519-763-5902. E-mail: ajwright@uoguelph.ca.

Notes

The authors declare no competing financial interest.

ACKNOWLEDGMENTS

We thank Robert Harris for his help with the transmission electron microscopy.

REFERENCES

(1) Muller, R. H.; Mader, K.; Gohla, S. Solid lipid nanoparticles (SLN) for controlled drug delivery - a review of the state of the art. *Eur. J. Pharm. Biopharm.* **2000**, *50*, 161−177.

(2) McClements, D. J. Nanoemulsions versus microemulsions: terminology, differences, and similarities. *Soft Matter* **2012**, *8*, 1719−1729.

(3) Bunjes, H.; Koch, M. H. J.; Westesen, K. Influence of emulsifiers on the crystallization of solid lipid nanoparticles. *J. Pharm. Sci.* **2003**, *92*, 1509−1520.

(4) Aronhime, J. S.; Sarig, S.; Garti, N. Dynamic control of polymorphic transformation in triglycerides by surfactants - the button syndrome. *J. Am. Oil Chem. Soc.* **1988**, *65*, 1144−1150.

(5) Bunjes, H.; Koch, M. H. J. Saturated phospholipids promote crystallization but slow down polymorphic transitions in triglyceride nanoparticles. *J. Controlled Release* **2005**, *107*, 229−243.

(6) Hou, D. Z.; Xie, C. S.; Huang, K. J.; Zhu, C. H. The production and characteristics of solid lipid nanoparticles (SLNs). *Biomaterials* **2003**, *24*, 1781−1785.

(7) Helgason, T.; Awad, T. S.; Kristbergsson, K.; McClements, D. J.; Weiss, J. Influence of polymorphic transformations on gelation of tripalmitin solid lipid nanoparticle suspensions. *J. Am. Oil Chem. Soc.* **2008**, *85*, 501−511.

(8) Trujillo, C. C.; Wright, A. J. Properties and stability of solid lipid particle dispersions based on canola stearin and poloxamer 188. *J. Am. Oil Chem. Soc.* **2010**, *87*, 715−730.

(9) Bunjes, H.; Westesen, K.; Koch, M. H. J. Crystallization tendency and polymorphic transitions in triglyceride nanoparticles. *Int. J. Pharm.* **1996**, *129*, 159−173.

(10) Rosenblatt, K. M.; Bunjes, H. Poly(vinyl alcohol) as emulsifier stabilizes solid triglyceride drug carrier nanoparticles in the a-modification. *Mol. Pharmaceutics* **2008**, *6*, 105−120.

(11) Jenning, V.; Schafer-Korting, M.; Gohla, S. Vitamin A-loaded solid lipid nanoparticles for topical use drug release properties. *J. Controlled Release* **2000**, *66*, 115−126.

(12) Helgason, T.; Awad, T. S.; Kristbergsson, K.; Decker, E. A.; McClements, D. J.; Weiss, J. Impact of surfactant properties on oxidative stability of beta-carotene encapsulated within solid lipid nanoparticles. *J. Agric. Food Chem.* **2009**, *57*, 8033−8040.

(13) Helgason, T.; Awad, T. S.; Kristbergsson, K.; McClements, D. J.; Weiss, J. Effect of surfactant surface coverage on formation of solid lipid nanoparticles (SLN). *J. Colloid Interface Sci.* **2009**, *334*, 75−81.

(14) Jores, K.; Mehnert, W.; Drechsler, M.; Bunjes, H.; Johann, C.; Mader, K. Investigations on the structure of solid lipid nanoparticles (SLN) and oil-loaded solid lipid nanoparticles by photon correlation spectroscopy, field-flow fractionation and transmission electron microscopy. *J. Controlled Release* **2004**, *95*, 217−227.

(15) Alexandridis, P.; Hatton, T. A. Poly(ethylene oxide)-poly-(propylene oxide)-poly(ethylene oxide) block-copolymer surfactants in aqueous-solutions and at interfaces - thermodynamics, structure, dynamics, and modeling. *Colloids Surf., A* **1995**, *96*, 1−46.

(16) Green, R. J.; Tasker, S.; Davies, J.; Davies, M. C.; Roberts, C. J.; Tendler, S. J. B. Adsorption of PEO-PPO-PEO triblock copolymers at the solid/liquid interface: A surface plasmon resonance study. *Langmuir* **1997**, *13*, 6510−6515.

(17) Boon, C. S.; Xu, Z.; Yue, X.; McClements, D. J.; Weiss, J.; Decker, E. A. Factors affecting lycopene oxidation in oil-in-water emulsions. *J. Agric. Food Chem.* **2008**, *56*, 1408−1414.

(18) McClements, D. J.; Decker, E. A. Lipid oxidation in oil-in-water emulsions: Impact of molecular environment on chemical reactions in heterogeneous food systems. *J. Food Sci.* **2000**, *65*, 1270−1282.

(19) Choubert, G.; Guillou, A.; Tyssandier, V.; Borel, P.; Grolier, P. Health value of carotenoids. *Sci. Aliments* **2001**, *21*, 467−480.

(20) Tan, C. P.; Nakajima, M. beta-Carotene nanodispersions: preparation, characterization and stability evaluation. *Food Chem.* **2005**, *92*, 661−671.

(21) Borel, P.; Grolier, P.; Armand, M.; Partier, A.; Lafont, H.; Lairon, D.; AzaisBraesco, V. Carotenoids in biological emulsions: Solubility, surface-to-core distribution, and release from lipid droplets. *J. Lipid Res.* **1996**, *37*, 250−261.

(22) McClements, D. J. Critical review of techniques and methodologies for characterization of emulsion stability. *Crit. Rev. Food Sci.* **2007**, *47*, 611−649.

(23) Khossravi, M.; Kao, Y. H.; Mrsny, R. J.; Sweeney, T. D. Analysis methods of polysorbate 20: A new method to assess the stability of polysorbate 20 and established methods that may overlook degraded polysorbate 20. *Pharm. Res.* **2002**, *19*, 634−639.

(24) Wright, A. J.; Pietrangelo, C.; MacNaughton, A. Influence of simulated upper intestinal parameters on the efficiency of beta carotene micellarisation using an in vitro model of digestion. *Food Chem.* **2008**, *107*, 1253−1260.

(25) Yin, L. J.; Chu, B. S.; Kobayashi, I.; Nakajima, M. Performance of selected emulsifiers and their combinations in the preparation of beta-carotene nanodispersions. *Food Hydrocolloids* **2009**, *23*, 1617−1622.

(26) McClements, D. J.; Dickinson, E.; Dungan, S. R.; Kinsella, J. E.; Ma, J. G.; Povey, M. J. W. Effect of emulsifier type on the crystallization kinetics of oil-in-water emulsions containing a mixture of solid and liquid droplets. *J. Colloid Interface Sci.* **1993**, *160*, 293−297.

(27) Santander-Ortega, M. J.; Jodar-Reyes, A. B.; Csaba, N.; Bastos-Gonzalez, D.; Ortega-Vinuesa, J. L. Colloidal stability of Pluronic F68-coated PLGA nanoparticles: A variety of stabilisation mechanisms. *J. Colloid Interface Sci.* **2006**, *302*, 522−529.

(28) Malaki Nik, A.; Corredig, M.; Wright, A. J. Release of lipophilic molecules during in vitro digestion of soy protein-stabilized emulsions. *Mol. Nutr. Food Res.* **2011**, *55*, S278−S289.

(29) Wulff-Perez, M.; Torcello-Gomez, A.; Galvez-Ruiz, M. J.; Martin-Rodriguez, A. Stability of emulsions for parenteral feeding: Preparation and characterization of o/w nanoemulsions with natural oils and Pluronic f68 as surfactant. *Food Hydrocolloids* **2009**, *23*, 1096−1102.

(30) Maskarinec, S. A.; Hannig, J.; Lee, R. C.; Lee, K. Y. C. Direct observation of poloxamer 188 insertion into lipid monolayers. *Biophys. J.* **2002**, *82*, 1453−1459.

(31) Hait, S. K.; Moulik, S. P. Determination of critical micelle concentration (CMC) of nonionic surfactants by donor-acceptor interaction with iodine and correlation of CMC with hydrophile-lipophile balance and other parameters of the surfactants. *J. Surfactants Deterg.* **2001**, *4*, 303−309.

(32) Souto, E. B.; Wissing, S. A.; Barbosa, C. M.; Muller, R. H. Development of a controlled release formulation based on SLN and NLC for topical clotrimazole delivery. *Int. J. Pharm.* **2004**, *278*, 71−77.

(33) Ruiz, C. C.; Molina-Bolivar, J. A.; Aguiar, J.; MacIsaac, G.; Moroze, S.; Palepu, R. Effect of ethylene glycol on the thermodynamic and micellar properties of Tween 20. *Colloid Polym. Sci.* **2003**, *281*, 531−541.

(34) Bunjes, H.; Steiniger, F.; Richter, W. Visualizing the structure of triglyceride nanoparticles in different crystal modifications. *Langmuir* **2007**, *23*, 4005−4011.

(35) Siekmann, B.; Westesen, K. Thermoanalysis of the recrystallization process of melt-homogenized glyceride nanoparticles. *Colloids Surf., B* **1994**, *3*, 159−175.

(36) Kuntsche, J.; Koch, M. H. J.; Steiniger, F.; Bunjes, H. Influence of stabilizer systems on the properties and phase behavior of supercooled smectic nanoparticles. *J. Colloid Interface Sci.* **2010**, *350*, 229−239.

(37) Hentschel, A.; Gramdorf, S.; Muller, R. H.; Kurz, T. Beta-carotene-loaded nanostructured lipid carriers. *J. Food Sci.* **2008**, *73*, N1−N6.

(38) Bunjes, H.; Drechsler, M.; Koch, M. H. J.; Westesen, K. Incorporation of the model drug ubidecarenone into solid lipid nanoparticles. *Pharm. Res.* **2001**, *18*, 287−293.

(39) Schubert, M. A.; Muller-Goymann, C. C. Characterisation of surface-modified solid lipid nanoparticles (SLN): Influence of lecithin and nonionic emulsifier. *Eur. J. Pharm. Biopharm.* **2005**, *61*, 77−86.

(40) Petersen, S.; Steiniger, F.; Fischer, D.; Fahr, A.; Bunjes, H. The physical state of lipid nanoparticles influences their effect on in vitro cell viability. *Eur. J. Pharm. Biopharm.* **2011**, *79*, 150−161.
(41) Kanasawud, P.; Crouzet, J. C. Mechanism of formation of volatile compounds by thermal-degradation of carotenoids in aqueous-medium. 1. beta-carotene degradation. *J. Agric. Food Chem.* **1990**, *38*, 237−243.
(42) Henry, L. K.; Catignani, G.; Schwartz, S. Oxidative degradation kinetics of lycopene, lutein, and 9-cis and all-trans beta-carotenee. *J. Am. Oil Chem. Soc.* **1998**, *75*, 823−829.
(43) McClements, D. J.; Decker, E. A.; Weiss, J. Emulsion-based delivery systems for lipophilic bioactive components. *J. Food Sci.* **2007**, *72*, R109−R124.